

Reductant Responsive Poly (N-Isopropylacrylamide) Microgels and Microgel-Based Optical Materials

Xue Li, Yongfeng Gao, Michael J. Serpe*

Department of Chemistry, University of Alberta, Edmonton, AB, Canada

*Corresponding Author: Michael J. Serpe (michael.serpe@ualberta.ca)

Keywords: Poly (N-Isopropylacrylamide)-based microgels, Colorimetric thiol detection, Microgel-based etalons, Stimuli responsive polymers

Abstract

Poly (N-isopropylacrylamide) (pNIPAm)-based hydrogel particles (microgels) crosslinked with N, N'-bis(acryloyl)cystamine (BAC) were prepared using free-radical precipitation polymerization. By coating a single layer of microgels on a Au-coated glass substrate followed by the addition of another Au layer, an optical device (etalon) was fabricated. The devices were shown to exhibit optical properties that are typical of microgel-based etalons, i.e., they exhibit visual color and unique multipeak reflectance spectra. Unique to the devices here are their ability to change their optical properties in the presence of thiols. Specifically, in the presence of dithiothreitol (DTT), the microgel crosslinks were reduced, leading to microgel swelling, which ultimately changes the optical properties of the etalon. We observed a linear relationship between the shift in the position of the reflectance peaks and the concentration of DTT, which suggests that they can be used to quantify thiols in solution.

Keywords Stimuli responsive polymers; Thiol detection; Photonic materials; Poly (N-Isopropylacrylamide); Etalons

23

24

25 **Introduction**

26 Stimuli responsive materials are capable of changing their chemical and/or physical properties in
27 response to specific changes in their environment.¹ A number of responsivities have been reported
28 previously, including responses to: pH,² temperature,^{3,4} light,⁵ and electric field.⁶ Ideally, these responses
29 are reversible, i.e., once the stimulus is removed, the responsive material returns to its initial state. These
30 materials have found a number of applications for controlled/triggered drug delivery,⁷⁻⁹ as antibacterial
31 coatings,^{10,11} and for tissue engineering.¹² While all of these responsivities have been previously reported,
32 thermoresponsive materials composed of poly (N-isopropylacrylamide) (pNIPAm) are the most widely
33 studied and best understood. Specifically, pNIPAm-based hydrogel particles (microgels) are fully water
34 soluble/swollen (and hydrophilic) in water with a temperature below pNIPAm's lower critical solution
35 temperature (LCST) of ~32 °C, while it transitions to an "insoluble"/deswollen (and relatively
36 hydrophobic) state when the water temperature is increased to above 32 °C. This behavior has been
37 exploited for many applications.^{13-19,20-22}

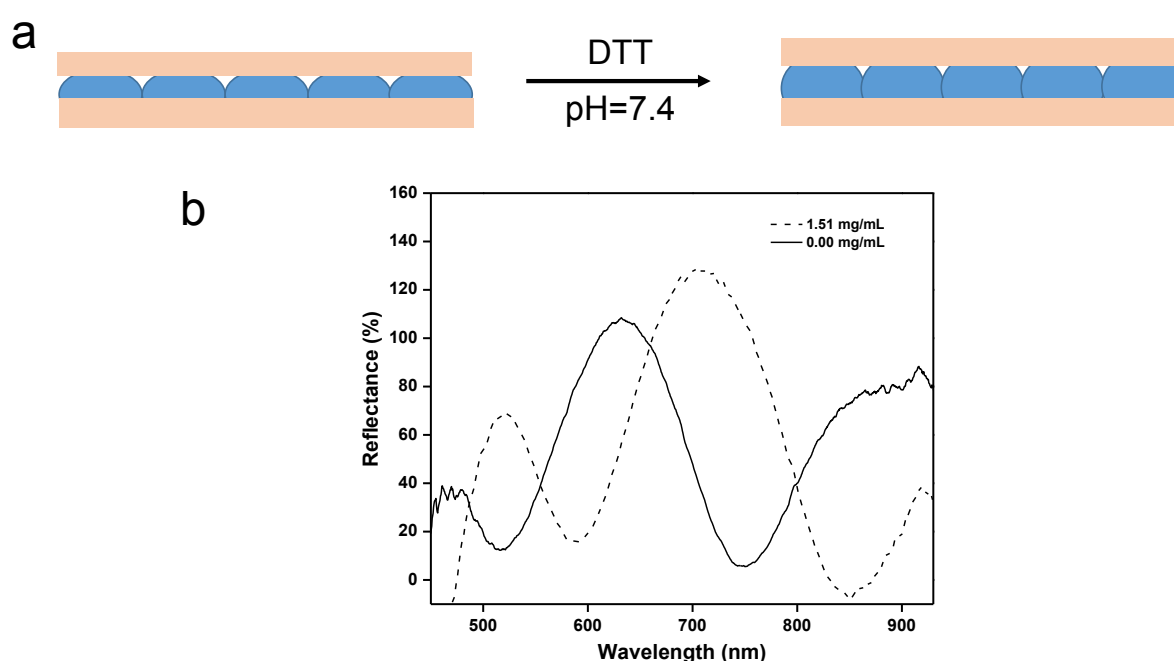
38 Previous work in the group has shown that an optical device (etalon) could be fabricated by
39 sandwiching a single layer of pNIPAm-based microgels between two thin metal layers. A schematic
40 depiction of the device, also known as an etalon, can be seen in Figure 1a. As can be seen in Figure 1b,
41 these devices exhibit unique multipeak reflectance spectra, which can be exploited for sensing
42 applications. The position of the peaks in the reflectance spectrum depends on the distance between the
43 device's two Au layers and the refractive index of microgels as shown in Equation (1).

44

$$\lambda_m = 2nd \cos\theta \quad (1)$$

45 where λ is the wavelength maximum of the peak(s), m is the peak order, n is the refractive index of the
46 dielectric, d is the spacing between the mirrors, and θ is the angle of incidence. Using this construct, we
47 have developed optical sensors that change their optical properties in response to glucose,²³
48 polyelectrolytes,²⁴ proteins,²⁵ light,²⁶ and pH.²⁷ This is a direct result of the microgel diameter modulating
49 the distance between the two metal layers.

50 In this work, we developed microgel-based optical sensors for thiols (dithiothreitol (DTT)), in solution.



51
52 Figure 1. (a) Schematic depiction of a microgel based etalon. A layer of pNIPAm-BAC microgels is
53 sandwiched between two Au layers. The microgels swell upon exposure to DTT, which increases the
54 distance between two Au layers. (b) A representative reflectance spectrum from a pNIPAm-BAC
55 microgel-based etalon both before and after DTT exposure.

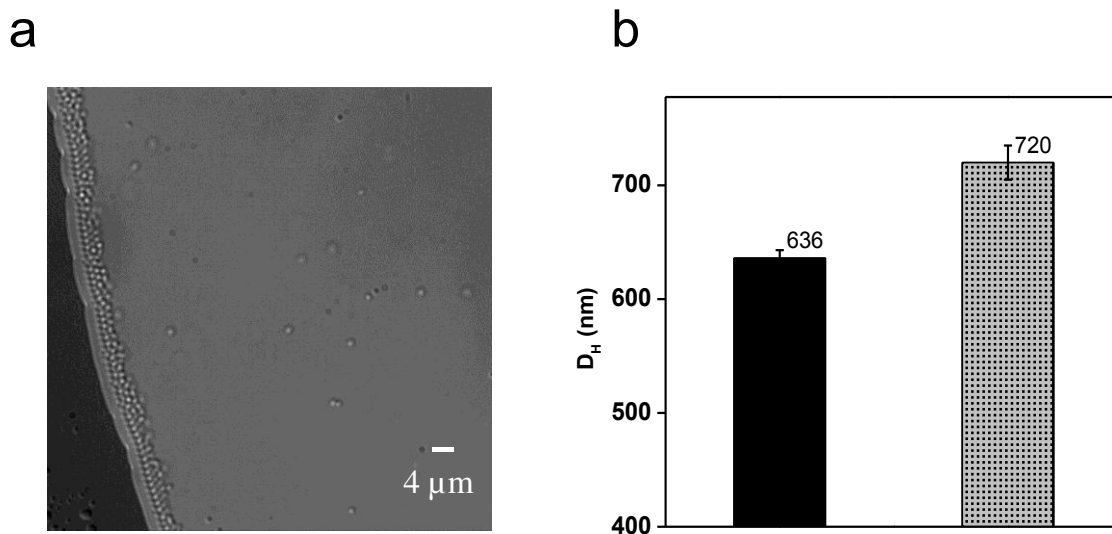
56
57 This was accomplished by synthesizing pNIPAm-based microgels, which were crosslinked with the
58 disulfide-based cross linker N, N'-bis(acryloyl)cystamine (BAC); these microgels were subsequently used
59 as the dielectric layer in an etalon.²⁸ We have shown that the BAC-crosslinked microgels exhibit a volume

60 change in the presence of DTT, which we attribute to the reduction of the BAC crosslinks, effectively
61 reducing the crosslink density. This change in volume leads to a change in the optical properties of the
62 sensors, which depended on the concentration of DTT.

63

64 **Results and Discussion**

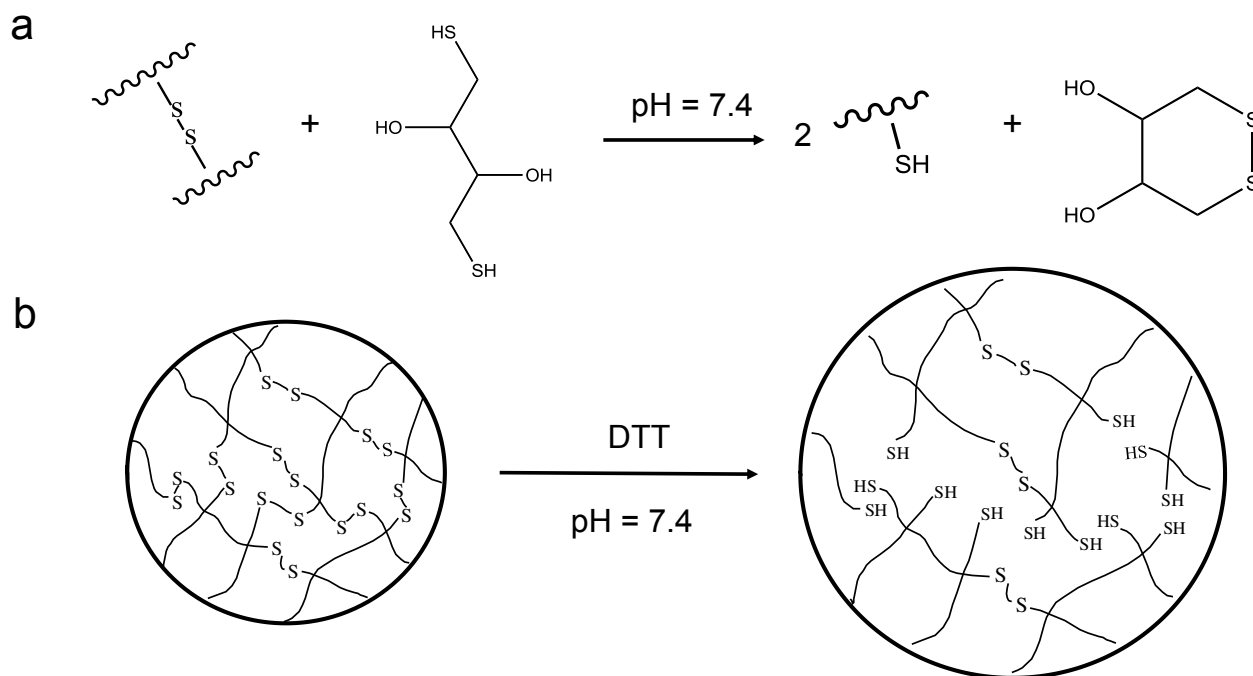
65 Free-radical precipitation polymerization was used to synthesize BAC crosslinked pNIPAm-based
66 microgels. As can be seen in the differential interference contrast (DIC) microscopy image in Figure 2a,
67 the microgels are monodispersed with an average diameter of ~900 nm (determined from the microscopy
68 images). In order to examine the BAC crosslinked microgels response to the presence of the reducing
69 agent DTT, we dispersed the microgels in 10 mM phosphate buffer solution (PBS) (pH = 7.4) containing
70 1 mg/mL DTT and determined their hydrodynamic diameter (D_H) via dynamic light scattering (DLS). As
71 shown in Figure 2b, the D_H of microgels in DTT solution is about 100 nm larger than in PBS alone. We
72 attributed this to the DTT reducing the BAC, which reduces the crosslink density, and therefore allows the
73 microgels to swell to a greater degree than before they were reduced. The reduction mechanism is shown
74 in Figure 3a. At pH 7.4, the DTT is negatively charged, and the negatively charged thiolate is reactive,
75 which can attack the disulfide bond in the microgel to generate thiols in the microgel and ring oxidized
76 DTT. As a result, the microgels will increase in diameter when the crosslinks are broken, as shown
77 schematically in Figure 3b.



78

79 Figure 2. (a) DIC microscope image for BAC crosslinked pNIPAm-based microgel particles; (b) D_H of
 80 BAC crosslinked pNIPAm-based microgel particles in the absence and presence of DTT.

81



82

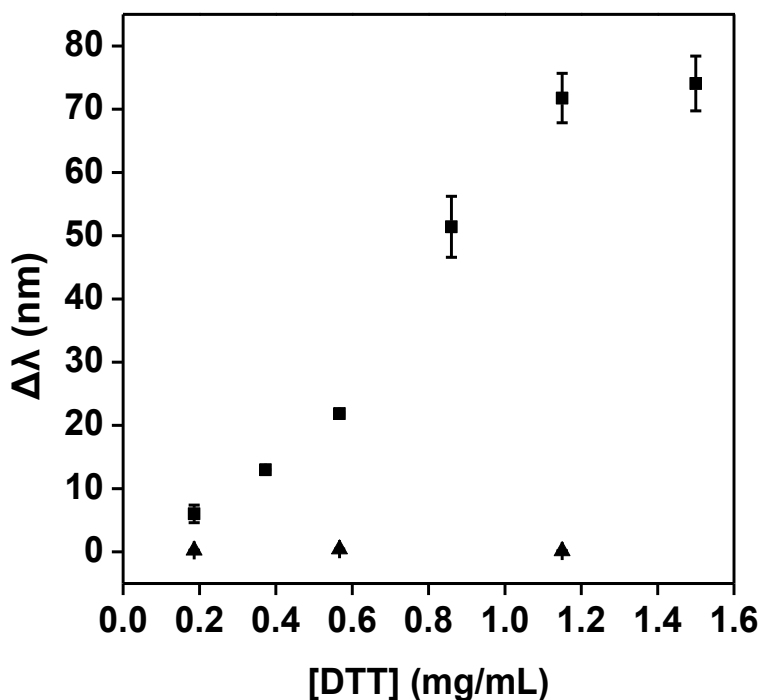
83 Figure 3. (a) The reduction mechanism of disulfide bond by DTT; (b) The proposed microgel swelling
 84 behavior after reduction of the microgel's BAC crosslinks.

85

86 Following the characterization of the microgels, we went on to show that microgel-based etalons could be
87 fabricated from the BAC crosslinked microgels. Again, a schematic representation of the microgel-based
88 etalon structure can be seen in Figure 1a. As we observed in solution above, the microgels increase in
89 diameter when DTT is introduced to the microgels; therefore, we expect similar behavior for the
90 microgels in the etalon. This swelling should result in an increase in the thickness of the dielectric layer,
91 yielding a red shift in the peaks of the reflectance spectrum, as can be predicted from Equation 1. To
92 study these materials, the DTT sensitive etalons were immersed in a 10 mM pH 7.4 phosphate buffer
93 solution at 25 °C. We exposed our etalons to different concentrations of DTT, and waited for the etalon
94 response to stabilize, which was ~ 1.5 h. Figure 1b shows a representative multippeak reflectance spectrum,
95 and the peaks clearly red shift as the concentration of DTT is increased. Figure 4 shows how the position
96 of the pNIPAm-BAC microgel-based etalons reflectance peak depends on the concentration of DTT. In
97 this figure $\Delta\lambda$ represents the reflectance peak wavelength shift of etalons in response to DTT. As can be
98 seen, the etalons show an average cumulative red shift of ~6 nm with 0.19 mg/mL solution. Successive
99 additions gave further red shifts and we observed ~70 nm shift over the range of concentration from 0.00
100 mg/mL to 1.50 mg/mL. Nevertheless, a control was also performed using pNIPAm-BIS microgels without
101 disulfide bonds inside in the same manner. As shown in Figure 4, they didn't exhibit red shifts after DTT
102 exposure. From the data we can conclude that the cleavage of disulfide bond by DTT can trigger the
103 volume change of the microgel by decreasing the crosslinking density, which results in a red shift of the
104 etalon's spectral peaks. Conclusively, the etalon device can be used as a powerful tool to detect the
105 reducing reagent DTT.

106

107



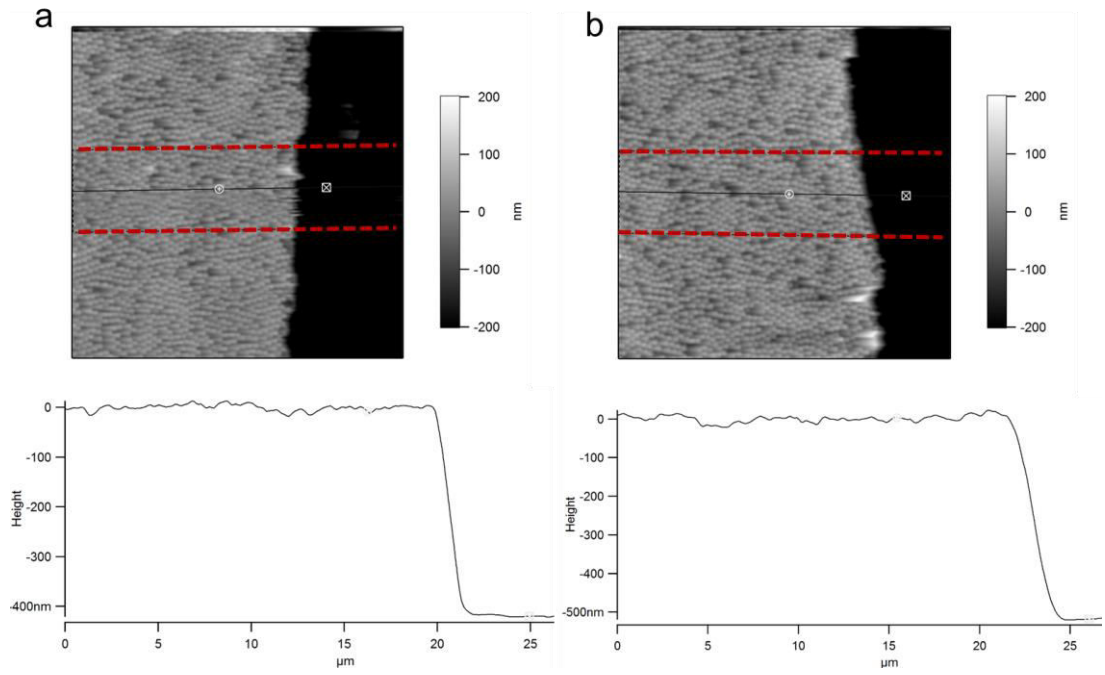
108

109 Figure 4. The squares represent the position of the etalons reflectance peak after exposure to the indicated
 110 amount of DTT; and the triangles represent the response of pNIPAm-BIS (no BAC) microgel-based
 111 etalons to DTT. Each point represents the average of three independent measurements from three etalons,
 112 and the error bars are the standard deviation for those values.

113

114 In the discussion above, we propose that the DTT is able to reduce the crosslink density of the BAC
 115 containing pNIPAm-based microgels, leading to their swelling. We propose that this swelling is capable
 116 of changing the optical properties of the microgel-based etalons, which can be used for sensing reducing
 117 agents (specifically DTT). To further prove this mechanism, we collected atomic force microscopy (AFM)
 118 images of BAC crosslinked pNIPAm microgel-based etalons in buffer without and with DTT present.
 119 From these images, we were able to determine the etalons thickness. To accomplish this, an etalon was
 120 formed on a substrate, as previously described, and was scratched with a razor blade to remove the etalon

121 from a specific area. The substrate was then imaged in the scratched region to determine the etalons
122 thickness before and after exposure to DTT. Figure 5a shows the AFM image for the etalon in the
123 scratched region after soaking in PBS with pH 7.4, and reveals a thickness of ~ 430 nm, which is expected
124 since previous studies have shown that the thickness of a microgel layer on a Au surface is significantly
125 thinner than expected solely from the solution diameter. Then the etalon was exposed to 1 mg/mL DTT in
126 the same PBS buffer for 2 h, followed by AFM imaging. Figure 5b shows the image for the etalon in the
127 same region as Figure 5a, which reveals a thickness of ~ 520 nm. These data correlate well with the
128 solution data, as well as the red shifts observed in the reflectance spectra.



129
130 Figure 5. AFM images of etalons in (a) pH 7.4 phosphate buffer solution; and (b) the same solution
131 containing 1 mg/mL DTT. The images were taken in a scratched region to allow easy determination of the
132 etalon thickness. The thickness was determined from average thicknesses determined in the step area in
133 the area bounded by the dashed lines. The analysis was carried out at 25 °C and revealed that the
134 thicknesses were (a) $423 \text{ nm} \pm 9 \text{ nm}$, and (b) $522 \text{ nm} \pm 15 \text{ nm}$.

136 **Conclusion**

137 In this work, we have shown that BAC crosslinked pNIPAm-based microgels could be synthesized, and
138 etalons made from them. We found that the microgel diameter depended on the presence of DTT, due to
139 the DTT reducing the BAC crosslinks, thereby decreasing the microgels crosslink density, which allows
140 them to swell. Color tunable device (etalons) were subsequently fabricated from these microgels by
141 sandwiching them between two Au layers. These devices exhibit optical properties, specifically multipeak
142 reflectance spectra, which were shown to depend on the presence and concentration of DTT they are
143 exposed to. Specifically, in response to DTT, the BAC crosslinked microgel etalons exhibit a reflectance
144 peak that shifts ~70 nm over the DTT concentration range of 0.19-1.5 mg/mL. Using AFM, we were able
145 to prove that this response was a result of the etalon's cavity thickness increasing, which leads to the
146 observed red shifts. From these results, we believe that thiol/DTT sensors can be fabricated from simple
147 components, and can also have applications for controlled and triggered drug delivery application.

148 **Experimental section**

149 **Materials.**

150 The monomer N-isopropylacrylamide (NIPAm) was recrystallized from hexanes and dried in vacuum
151 prior to use. Reagents N, N'-bis(acryloyl)cystamine (BAC), N, N'-methylene bis(acrylamide) (BIS),
152 ammonium persulfate (APS), dithiothreitol (DTT), methanol, monosodium phosphate were all used as
153 received. All deionized water was 18.2 M Ω ·cm and obtained from a Milli-Q Plus system from Millipore
154 (Billerica, MA). Glass cover slips were 25 mm \times 25 mm and obtained from Fisher Scientific. Cr was
155 99.999% and obtained from ESPI (Ashland OR), while Au was 99.99% and obtained from MRCS Canada
156 (Edmonton, AB). Au annealing was performed in an Isotemp muffle furnace from Fisher Scientific
157 (Ontario, Canada).

158

159 Microgel synthesis.

160 A 3-necked round bottom flask was fitted with a reflux condenser, a nitrogen inlet (needle) and
161 temperature probe, and charged with a solution of NIPAm (1.767 mmol) in 20 mL DI water, previously
162 filtered through a 0.2 μm filter. The solution was purged with N_2 gas and allowed to heat to $\sim 70^\circ\text{C}$ for ~ 1
163 hour. The reaction was initiated with a solution of 0.1 M APS (total concentration 0.4 mM), immediately
164 after addition of 4.63 mM BAC dissolved in 5 mL methanol. The solution was allowed to stir at $\sim 70^\circ\text{C}$
165 for 6 h, then cooled to room temperature and filtered to remove large aggregates. These microgels were
166 then centrifuged at a speed of ~ 8000 relative centrifugal force (rcf) at room temperature for 35 mins to
167 form a pellet at the bottom of centrifuge tubes. The supernatant was removed and the pellets of microgels
168 were resuspended using deionized water. This process was repeated for six times to remove any
169 remaining monomers and linear polymers. NIPAm-co-BIS was synthesized as previously described.²⁸

170

171 Etalon fabrication.

172 Etalons were fabricated according to the procedures reported elsewhere.²⁸ Briefly, 25×25 mm glass
173 coverslips were rinsed with DI water and ethanol and dried with N_2 gas. 2 nm of Cr followed by 15 nm of
174 Au were thermally evaporated onto the glass at a rate of ~ 0.1 and $\sim 0.25 \text{ \AA s}^{-1}$, respectively, using a Torr
175 International Inc. model THEUPG thermal evaporation system (New Windsor, NY). The Cr acts as an
176 adhesion layer to hold the Au layer on the glass. The Au coated substrates were annealed at 250°C for 3 h
177 and then cooled to room temperature prior to use. Then a previously coated Cr/Au substrate was rinsed
178 with ethanol, dried with N_2 , and then placed onto hot plate (Corning, NY) at $\sim 30^\circ\text{C}$. A 40 μL aliquot of
179 the concentrated microgels was spread to cover the whole substrate using a micropipette tip. Then the

180 microgel solution was allowed to completely dry on the substrate at ~35 °C for 2 h. After that, the dry
181 film was rinsed copiously with DI water and soaked in water overnight at ~30 °C. Following this step,
182 the substrate was again rinsed with DI water and dried with N₂ gas, and an additional 2 nm Cr and 15 nm
183 Au overlayer were deposited onto the microgel layer.

184

185 Reflectance spectroscopy.

186 Reflectance spectra were collected by a USB 2000+ spectrophotometer, connecting with light source and
187 a reflectance probe from Ocean Optics (Dunedin FL). A Corning PC-420d hot plate (Fisher, Ottawa,
188 Ontario) was used to control the solution temperature and the temperature was also monitored with a
189 thermocouple platinum sensor. The spectra were collected over a wavelength range of 400-1000 nm and
190 analyzed by Ocean Optics Spectra Suite Spectroscopy software.

191

192 Particle characterization.

193 The morphology of microgel particles were investigated by Differential Interference Contrast (DIC)
194 images via IX71 inverted microscope (Olympus, Japan). Dynamic light scattering (DLS) was carried out
195 to determine the hydrodynamic diameter of the microgels using a Zetasizer Nano ZS equipped with a 633
196 nm laser (Malvern, Westborough, MA, USA) and measured in 173° backscatter mode. All measurements
197 of hydrodynamic diameter was repeated three times.

198

199 Atomic force microscopy (AFM) tapping imaging.

200 In-liquid height analysis for a BAC crosslinked pNIPAm microgel-based etalons was done in pH 7.4
201 phosphate buffer solution before and after DTT exposure. The images were obtained using an Asylum

202 Research MFP 3D AFM (Santa Barbara, CA). Images were acquired over a 30 ×30 μm area using a scan
203 rate of 0.50 Hz. For this analysis, a line was scratched into the etalon using a razor blade and the scratch
204 was imaged. Images were first taken in pH 7.4 phosphate buffer solution at 25 °C. Then the sample was
205 treated in 1 mg/mL DTT phosphate buffer solution for at least 2 h. After that, the sample was imaged
206 using the same method at 25 °C. The height was determined using Asylum software.

207

208 **Acknowledgements**

209 MJS acknowledges funding from the University of Alberta (the Department of Chemistry and the Faculty
210 of Science), the Natural Sciences and Engineering Research Council of Canada (NSERC), the Canada
211 Foundation for Innovation (CFI), the Alberta Advanced Education & Technology Small Equipment
212 Grants Program (AET/SEGP), IC-IMPACTS and Grand Challenges Canada.

213

214 **Reference**

215

216

217

- 218 (1) Theato, P.; Sumerlin, B. S.; O'Reilly, R. K.; Epps, III T. H. *Chem. Soc. Rev.* **2013**, *42*, 7055.
- 219 (2) Hoare, T.; Pelton, R. *Macromolecules* **2004**, *37*, 2544.
- 220 (3) Lyon, L. A.; Meng, Z. Y.; Singh, N.; Sorrell, C. D.; John, A. S. *Chem. Soc. Rev.* **2009**, *38*, 865.
- 221 (4) Pelton, R. *Adv. Colloid Interface Sci.* **2000**, *85*, 1.
- 222 (5) Suzuki, A.; Tanaka, T. *Nature* **1990**, *346*, 345.
- 223 (6) Tanaka, T.; Nishio, I.; Sun, S. T.; Uenonishio, S. *Science* **1982**, *218*, 467.
- 224 (7) Schmaljohann, D. *Adv. Drug Deliv. Rev.* **2006**, *58*, 1655.
- 225 (8) Ganta, S.; Devalapally, H.; Shahiwala, A.; Amiji, M. J. *Controlled Release* **2008**, *126*, 187.
- 226 (9) Islam, M. R.; Gao, Y.; Li, X.; Serpe, M. J. *J. Mater. Chem. B* **2014**, *2*, 2444.
- 227 (10) Cheng, G.; Xue, H.; Li, G.; Jiang, S. *Langmuir* **2010**, *26*, 10425.
- 228 (11) Zhou, C.; Li, P.; Qi, X.; Sharif, A. R. M.; Poon, Y. F.; Cao, Y.; Chang, M. W.; Leong, S. S. J.;
229 Chan- Park, M. B. *Biomaterials* **2011**, *32*, 2704.

- 230 (12) Lee, K. Y.; Mooney, D. J. *Chem. Rev.* **2001**, *101*, 1869.
- 231 (13) Reese, C. E.; Mikhonin, A. V.; Kamenjicki, M.; Tikhonov, A.; Asher, S. A. *J. Am. Chem. Soc.*
232 **2004**, *126*, 1493.
- 233 (14) Qiu, Y.; Park, K. *Adv. Drug Deliv. Rev.* **2001**, *53*, 321.
- 234 (15) Wu, C.; Zhou, S. *Macromolecules* **1995**, *28*, 8381.
- 235 (16) Hoare, T.; Pelton, R. *Macromolecules* **2007**, *40*, 670.
- 236 (17) Gao, J.; Wu, C. *Macromolecules* **1997**, *30*, 6873.
- 237 (18) Alexeev, V. L.; Sharma, A. C.; Goponenko, A. V.; Das, S.; Lednev, I. K.; Wilcox, C. S.; Finegold,
238 D. N.; Asher, S. A. *Anal. Chem.* **2003**, *75*, 2316.
- 239 (19) Zhang, J.-T.; Smith, N.; Asher, S. A. *Anal. Chem.* **2012**, *84*, 6416.
- 240 (20) Saunders, B. R.; Vincent, B. *Adv. Colloid Interface Sci.* **1999**, *80*, 1.
- 241 (21) Islam, M. R.; Lu, Z.; Li, X.; Sarker, A. K.; Hu, L.; Choi, P.; Li, X.; Hakobyan, N.; Serpe, M. J.
242 *Anal. Chim. Acta* **2013**, *789*, 17.
- 243 (22) Ringsdorf, H.; Simon, J.; Winnik, F. M. *Macromolecules* **1992**, *25*, 7306.
- 244 (23) Sorrell, C.; Serpe, M. *Anal. Bioanal. Chem.* **2012**, *402*, 2385.
- 245 (24) Islam, M. R.; Serpe, M. J. *Macromolecules* **2013**, *46*, 1599.
- 246 (25) Islam, M. R.; Serpe, M. J. *Chem. Commun.* **2013**, *49*, 2646.
- 247 (26) Zhang, Q. M.; Xu, W.; Serpe, M. J. *Angew. Chem. Int. Ed.* **2014**, *53*, 4827.
- 248 (27) Hu, L.; Serpe, M. J. *J. Mater. Chem.* **2012**, *22*, 8199.
- 249 (28) Sorrell, C. D.; Carter, M. C. D.; Serpe, M. J. *Adv. Funct. Mater.* **2011**, *21*, 425.
- 250
- 251